Acta Crystallographica Section B
Structural Science, Crystal Engineering and Materials
ISSN 2052-5206

Metal-organic frameworks based on uranyl and phosphonate ligands

Bernardo Monteiro,[a] José A. Fernandes,[b] Cláudia C. L. Pereira,[a] Sérgio M. F. Vilela,[b] João P. C. Tomé,[c,d] Joaquim Marçalo[a] and Filipe A. Almeida Paz[b]*

[a]Centro de Ciências e Tecnologias Nucleares, Instituto Superior Técnico, Universidade de Lisboa, 2695-066 Bobadela LRS, Portugal, [b]CICECO, Departamento de Química, Universidade de Aveiro, Campus Universitário de Santiago, 3810-193 Aveiro, Portugal, [c]QOPNA, Departamento de Química, Universidade de Aveiro, Campus Universitário de Santiago, 3810-193 Aveiro, Portugal, and [d]Department of Organic Chemistry, Ghent University, B-9000 Ghent, Belgium

Correspondence e-mail: filipe.paz@ua.pt

Received 19 September 2013
Accepted 28 December 2013

Three new crystalline metal-organic frameworks have been prepared from the reaction of uranyl nitrate with nitrilotris(methylphosphonic acid) [H_6nmp, $N(CH_2PO_3H_2)_3$], 1,4-phenylenebis(methylene)diphosphonic acid [H_4pmd, $C_6H_4(PO_3H_2)_2$], and (benzene-1,3,5-triyltris(methylene))triphosphonic acid [H_6bmt, $C_6H_3(PO_3H_2)_3$]. Compound $[(UO_2)_2F(H_3nmp)(H_2O)]\cdot 4H_2O$ (I) crystallizes in space group $C2/c$, showing two crystallographically independent uranyl centres with pentagonal bipyramidal coordination geometries. While one metal centre is composed of a $\{(UO_2)O_3(\mu\text{-}F)\}_2$ dimer, the other comprises an isolated $\{(UO_2)O_5\}$ polyhedron. Compound $[(UO_2)(H_2pmd)]$ (II) crystallizes in space group $P2_1/c$, showing a centrosymmetric uranyl centre with an octahedral $\{(UO_2)O_4\}$ coordination geometry. Compound $[(UO_2)_3(H_3bmt)_2(H_2O)_2]\cdot 14H_2O$ (III) crystallizes in space group $P\bar{1}$, showing two crystallographically independent uranyl centres. One uranyl centre is a $\{(UO_2)O_5\}$ pentagonal bipyramid similar to that in (I), while the other is a $\{(UO_2)O_4\}$ centrosymmetric octahedron similar to that in (II). Compounds (I) and (III) contain solvent-accessible volumes accounting for *ca* 23.6 and 26.9% of their unit-cell volume, respectively. In (I) the cavity has a columnar shape and is occupied by disordered water molecules, while in (III) the cavity is a two-dimensional layer with more ordered water molecules. All compounds have been studied in the solid state using FT-IR spectroscopy. Topological studies show that compounds (I) and (III) are trinodal, with 3,6,6- and 4,4,6-connected networks, respectively. Compound (II) is instead a 4-connected uninodal network of the type **cds**.

1. Introduction

Metal-organic frameworks (MOFs) are nowadays typically prepared using hydrothermal synthetic approaches with the aim of obtaining crystalline products, in particular suitable large crystals for single-crystal diffraction. Most metal-organic assemblies involving *f*-block elements (Andrews & Cahill, 2013) make use of polycarboxylate ligands, particularly those built around an aromatic skeleton which are, by themselves, a particularly notable subset (Thuéry *et al.*, 2013). Our research group has been employing multipodal phosphonate-based organic linkers for the construction of MOFs with, mainly, rare-earth cations (Rocha *et al.*, 2009; Cunha-Silva, Ananias *et al.*, 2009; Cunha-Silva, Lima *et al.*, 2009; Soares-Santos *et al.*, 2010; Almeida Paz *et al.*, 2004, 2005; Shi, Paz, Girginova, Amaral *et al.*, 2006; Shi, Paz, Girginova, Rocha *et al.*, 2006; Vilela, Mendes *et al.*, 2013; Shi *et al.*, 2008; Silva *et al.*, 2011; Cunha-Silva *et al.*, 2007; Silva *et al.*, 2012; Vilela *et al.*, 2012; Vilela, Firmino *et al.*, 2013). The phosphonate group consti-

tutes a suitable rigid building block for the construction of robust multi-dimensional networks because the existence of three O atoms placed at the vertices of a tetrahedron mimics well the basic building unit of zeolites and zeo-type materials. These units are, in this way, structurally and thermally more robust than carboxylates, ultimately leading to stronger connections with larger cations such as uranyl. Phosphonate-based MOFs are, nevertheless, considerably fewer in the literature than their carboxylate-based counterparts. This is due in part to the fact that phosphonates tend to form densely packed layered structures that are not porous. In addition, because of their lower solubility, metal phosphonates tend to be less crystalline than carboxylates. This often means that even if a phosphonate-based MOF is obtained, it must be structurally characterized by powder X-ray diffraction (PXRD) instead of single-crystal methods (Adelani *et al.*, 2011). Notwithstanding, phosphonates have become a prominent family of ligands among those used in the synthesis of uranyl-organic frameworks (UOFs). Indeed, several groups have exploited the high affinity of phosphonic acids for uranyl to generate a large variety of original architectures, from one-dimensional nanotubules up to three-dimensional frameworks (Thuéry, 2013).

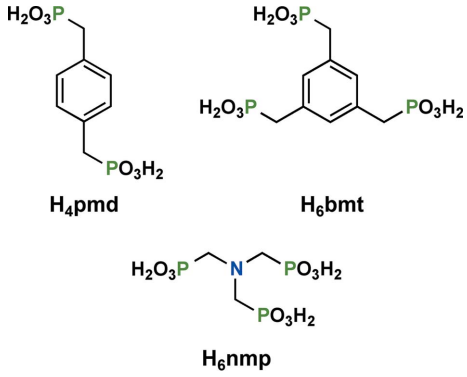

The richness in the structural chemistry of uranyl arises from the extremely flexible coordination chemistry of the uranyl cation, UO_2^{2+}, commonly adopting the UO_7 pentagonal bipyramidal geometry, but also yielding the less common UO_6 tetragonal bipyramid and the UO_8 hexagonal bipyramid (Alsobrook *et al.*, 2011). In this current work, we have employed $UO_2(NO_3)_2{\cdot}6H_2O$ as the source of uranyl and three organic polyphosphonate linkers already used by us, namely 1,4-phenylenebis(methylene)diphosphonic acid (H_4pmd) (Vilela, Mendes *et al.*, 2013; Shi *et al.*, 2008), nitrilotris(methylphosphonic acid) (H_6nmp) (Silva *et al.*, 2011, 2012; Cunha-Silva *et al.*, 2007) and (benzene-1,3,5-triyltris(methylene))triphosphonic acid (H_6bmt) (Vilela *et al.*, 2012; Vilela, Firmino *et al.*, 2013). Three new structures have been isolated and characterized, $[(UO_2)_2F(H_3nmp)(H_2O)]{\cdot}4H_2O$ (I), $[(UO_2)(H_2pmd)]$ (II) and $[(UO_2)_3(H_3bmt)_2(H_2O)_2]{\cdot}14H_2O$ (III), with phase purity being confirmed using a combination of elemental analyses and FT-IR spectroscopy.

2. Experimental

2.1. Materials and methods

The organic ligand nitrilotris(methylenephosphonic acid) [H_6nmp, $N(CH_2PO_3H_2)_3$, 97%, Fluka] is commercially available. 1,4-Phenylenebis(methylene)diphosphonic acid (H_4pmd; Vilela, Mendes *et al.*, 2013) and (benzene-1,3,5-triyltris(methylene))triphosphonic acid (H_6bmt; Vilela *et al.*, 2012) were prepared according to published procedures.

Elemental analysis (CHN) was performed on a CE Instruments EA1110 automatic analyser. To guarantee complete combustion of the samples, a couple of milligrams of V_2O_5 were added during the analysis, and the results were corrected to reflect the addition of this substance. FT-IR spectra (range 4000 350 cm^{-1}) were collected as KBr pellets (Sigma-Aldrich, FT-IR grade) using a Bruker Tensor 27 spectrometer by averaging 200 scans at a maximum resolution of 4 cm^{-1}.

2.2. Hydrothermal synthesis

Crystals of compounds (I) (III) were isolated by mixing $UO_2(NO_3)_2{\cdot}6H_2O$ and the appropriate organic ligand in deionized water (see below for the employed amounts). The reaction mixtures were then transferred into Teflon-lined 26 ml autoclaves that were placed at 363 K for a period of 15 h. A few drops of HF were added to the reaction mixtures to promote the isolation of phase-pure compounds (I) and (III). The addition of this mineralizing agent was not necessary for the preparation of crystalline compound (II).

2.2.1. $[(UO_2)_2F(H_3nmp)(H_2O)]{\cdot}4H_2O$ (I). 150.0 mg of $UO_2(NO_3)_2{\cdot}6H_2O$ (0.299 mmol) and 59.8 mg of the ligand H_6nmp (0.200 mmol) composed the initial reaction mixture. Elemental analysis: calc (%): C 3.81, H 2.03, N 1.48; found: C 3.99, H 2.38, N 1.47.

2.2.2. $[(UO_2)(H_2pmd)]$ (II). 150.0 mg of $UO_2(NO_3)_2{\cdot}6H_2O$ (0.299 mmol) and 79.6 mg of the ligand H_4pmd (0.299 mmol) composed the initial reaction mixture. Elemental analysis: calc (%): C 17.99, H 1.89; found: C 18.20, H 2.03.

2.2.3. $[(UO_2)_3(H_3bmt)_2(H_2O)_2]{\cdot}14H_2O$ (III). 150.0 mg $UO_2(NO_3)_2{\cdot}6H_2O$ (0.299 mmol) and 106.0 mg of the ligand H_6bmt (0.294 mmol) composed the initial reaction mixture. Elemental analysis: calc (%): C 11.93, H 3.11; found: C 12.10, H 3.32.

2.3. Single-crystal X-ray diffraction

Single crystals of (I) and (III) were harvested from the crystallization vials and immediately immersed in highly viscous FOMBLIN Y perfluoropolyether vacuum oil (LVAC 140/13, Sigma-Aldrich) to avoid degradation caused by evaporation of the solvent. Single crystals of (II) were harvested from the crystallization vials and immersed in silicon grease. All crystals were mounted on Hampton Research CryoLoops with the help of a Stemi 2000 stereomicroscope equipped with Carl Zeiss lenses (Kottke & Stalke, 1993). Data were collected on a Bruker X8 Kappa APEX-II CCD area-detector diffractometer (graphite-monochromated Mo $K\alpha$ radiation, λ = 0.7107 Å) equipped with an Oxford

Table 1
Experimental details.

Experiments were carried out with Mo $K\alpha$ radiation using a Bruker X8 Kappa CCD APEX-II diffractometer. Absorption was corrected for by multi-scan methods, *SADABS* (Bruker, 2008). H atoms were treated by a mixture of independent and constrained refinement.

	(I)	(II)	(III)
Crystal data			
Chemical formula	$C_3H_{11}FNO_{14}P_3U_2\cdot 4H_2O$	$C_8H_{10}O_8P_2U$	$C_9H_{14}O_{13}P_3U_{1.50}\cdot 7H_2O$
M_r	945.16	534.13	906.27
Crystal system, space group	Monoclinic, $C2/c$	Monoclinic, $P2_1/c$	Triclinic, $P\overline{1}$
Temperature (K)	150	296	150
a, b, c (Å)	25.8297 (10), 8.7560 (3), 17.7432 (7)	10.9522 (13), 6.4691 (7), 9.2802 (10)	8.7982 (3), 11.8876 (4), 12.6446 (4)
α, β, γ (°)	90, 99.951 (2), 90	90, 96.333 (9), 90	95.219 (2), 106.752 (2), 96.980 (2)
V (Å^3)	3952.5 (3)	653.50 (13)	1245.89 (7)
Z	8	2	2
μ (mm^{-1})	16.71	12.69	10.03
Crystal size (mm)	0.05 × 0.03 × 0.01	0.03 × 0.02 × 0.01	0.02 × 0.02 × 0.01
Data collection			
T_{min}, T_{max}	0.489, 0.921	0.702, 0.939	0.825, 0.906
No. of measured, independent and observed [$I > 2\sigma(I)$] reflections	76 767, 5310, 4724	8989, 2475, 1556	54 948, 4560, 4004
R_{int}	0.074	0.055	0.064
$(\sin\theta/\lambda)_{max}$ (Å^{-1})	0.685	0.769	0.602
Refinement			
$R[F^2 > 2\sigma(F^2)]$, $wR(F^2)$, S	0.026, 0.059, 1.06	0.034, 0.060, 1.00	0.021, 0.041, 1.08
No. of reflections	5310	2475	4560
No. of parameters	255	91	380
No. of restraints	5	1	32
$\Delta\rho_{max}$, $\Delta\rho_{min}$ (e Å^{-3})	1.52, 1.04	1.91, 2.74	0.63, 0.76

Computer programs: *APEX2* (Bruker, 2008), *SAINT-Plus* (Bruker, 2008), *SAINT-Plus, SHELXS97* (Sheldrick, 2008), *SHELXL97* (Sheldrick, 2008), *DIAMOND* (Brandenburg, 2009), *SHELXTL* (Bruker, 2008).

Cryosystems Series 700 Cryostream monitored remotely using the software interface *Cryopad* (Oxford Cryosystems, 2006).

Some O atoms of the crystallization water molecules [all in compound (I) and two in compound (III)] were refined with a common isotropic displacement parameter. The remaining non-H atoms were successfully refined using anisotropic displacement parameters. H atoms bound to C were placed at idealized positions and allowed to ride during refinement with $U_{iso}(H) = 1.2U_{eq}(C)$. H atoms bound to O or N [in (I)] belonging to the organic ligands were located from difference Fourier maps and refined with the O H and N H distances restrained to 0.95 (1) Å. In some cases, additional anti-bumping restraints were added, namely P···H greater than 2.00 (1) Å in (I), and H···H greater than 2.16 (1) Å for atoms belonging to different water molecules in (III). The H atom bound to O8 in (I) was included as disordered over two different positions with assigned site occupancies of 0.5. H atoms belonging to the anisotropically refined water molecules in (III) were also located from difference Fourier maps and refined with the O H and H···H distances restrained to 0.95 (1) and 1.55 (1) Å, respectively. The H atoms of the water molecules in (I) could not be located, and the atom sites in the structure are therefore 10 H atoms per formula unit (80 per unit cell) short of the stated compound formula.

The final difference Fourier synthesis for the three compounds showed: for (I), the highest peak (1.52 e Å^{-3}) located 0.94 Å from U1 and the deepest hole (−1.04 e Å^{-3}) 1.00 Å from U2; for (II), the highest peak (1.91 e Å^{-3}) and the deepest hole (−2.74 e Å^{-3}) located 0.48 and 0.77 Å from U1, respectively; for (III), the highest peak (0.64 e Å^{-3}) located 0.17 Å from O2*W* and the deepest hole (−0.76 e Å^{-3}) 0.86 Å from U2. Details of the crystallographic data collection and structure refinement are summarized in Table 1.[1]

3. Results

3.1. Crystal structure of $[(UO_2)_2F(H_3nmp)(H_2O)]\cdot 4H_2O$ (I)

Compound (I) crystallizes in space group $C2/c$, with the asymmetric unit being composed of a whole residue of nitrilotris(methylenephosphonic acid) (H_3nmp^{3-}), two crystallographically independent uranyl centres, a coordinated water molecule, a coordinated fluoride anion and four water molecules distributed among ten distinct crystallographic locations with fractional site occupancies (Fig. 1*a*). The presence of fluoride in the structure was proven by the combination of data arising from different characterization methods: on the one hand, the usage of a few drops of HF in the synthesis is crucial (see §2), since elimination of this step fails to lead to the same compound; on the other hand, both the elemental analysis and the performed crystallographic studies unequivocally show that these anions are present.

The coordination geometries around the metal centres resemble slightly distorted pentagonal bipyramids, with the oxo groups occupying the apical positions (see Table 2 for details). The equatorial positions of the coordination poly-

[1] Supporting information for this paper is available from the IUCr electronic archives (Reference: BI5030).

Table 2
Selected bond lengths and angles (Å, °) for the U^{6+} coordination environments in (I).

U1	O10	1.764 (4)	U2	O13	1.767 (4)
U1	O11	1.769 (4)	U2	O12	1.770 (4)
U1	O4	2.323 (4)	U2	O5	2.307 (3)
U1	O1	2.331 (4)	U2	$O6^{iii}$	2.311 (3)
U1	$O9^{i}$	2.354 (4)	U2	F1	2.351 (3)
U1	$O2^{ii}$	2.368 (4)	U2	$F1^{iv}$	2.336 (3)
U1	O1*W*	2.510 (4)	U2	$O7^{i}$	2.355 (4)
			U2···$U2^{iv}$		3.9829 (3)
O10	U1 O11	177.74 (19)	O13	U2 O12	179.02 (17)
O10	U1 O4	84.27 (17)	O13	U2 O5	88.77 (15)
O11	U1 O4	97.91 (17)	O12	U2 O5	91.88 (15)
O10	U1 O1	95.15 (17)	O13	U2 $O6^{iii}$	89.78 (15)
O11	U1 O1	86.01 (16)	O12	U2 $O6^{iii}$	91.04 (16)
O4	U1 O1	75.54 (13)	O5	U2 $O6^{iii}$	79.54 (12)
O10	U1 $O9^{i}$	93.82 (17)	O13	U2 $F1^{iv}$	90.48 (14)
O11	U1 $O9^{i}$	86.23 (17)	O12	U2 $F1^{iv}$	88.57 (15)
O4	U1 $O9^{i}$	73.50 (13)	O5	U2 $F1^{iv}$	146.73 (11)
O1	U1 $O9^{i}$	146.64 (13)	$O6^{iii}$	U2 $F1^{iv}$	133.72 (11)
O10	U1 $O2^{ii}$	85.63 (17)	O13	U2 F1	88.66 (14)
O11	U1 $O2^{ii}$	92.70 (17)	O12	U2 F1	91.14 (15)
O4	U1 $O2^{ii}$	151.51 (14)	O5	U2 F1	149.54 (11)
O1	U1 $O2^{ii}$	78.94 (13)	$O6^{iii}$	U2 F1	70.11 (11)
$O9^{i}$	U1 $O2^{ii}$	133.83 (13)	$F1^{iv}$	U2 F1	63.63 (11)
O10	U1 O1*W*	88.73 (18)	O13	U2 $O7^{i}$	90.02 (15)
O11	U1 O1*W*	89.24 (17)	O12	U2 $O7^{i}$	89.43 (16)
O4	U1 O1*W*	137.52 (13)	O5	U2 $O7^{i}$	76.57 (12)
O1	U1 O1*W*	146.92 (13)	$O6^{iii}$	U2 $O7^{i}$	156.11 (12)
$O9^{i}$	U1 O1*W*	65.24 (13)	$F1^{iv}$	U2 $O7^{i}$	70.17 (11)
$O2^{ii}$	U1 O1*W*	68.60 (13)	F1	U2 $O7^{i}$	133.77 (11)

Symmetry codes: (i) x, $y+1, z+\frac{1}{2}$; (ii) $x+1, y$, $z+\frac{1}{2}$; (iii) $x+\frac{1}{2}, y$ $\frac{1}{2}$, $z+\frac{1}{2}$; (iv) $x+\frac{1}{2}$, $y+\frac{1}{2}$, $z+1$.

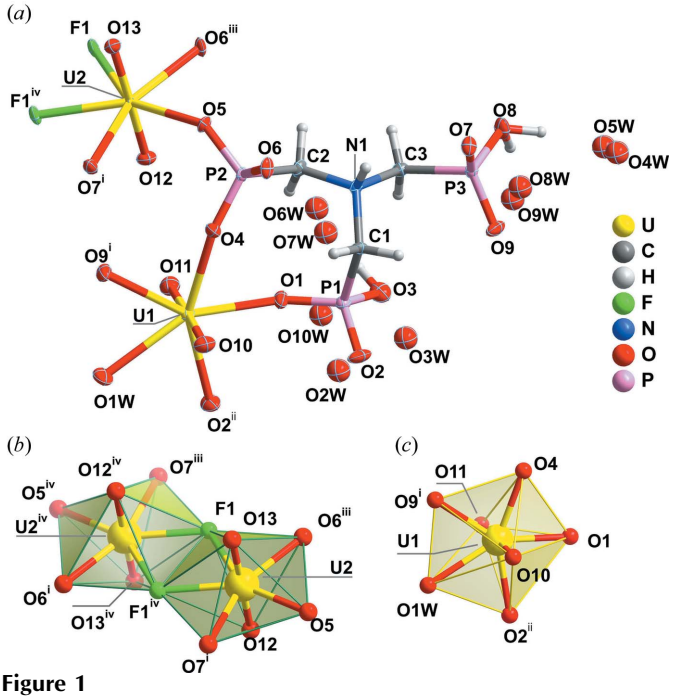

Figure 1
(*a*) Molecular units in (I). Non H atoms are represented as displacement ellipsoids drawn at 50% probability, while H atoms are represented as small spheres with arbitrary radii. Atom O8 is bonded to two H atoms, each with site occupancy 0.50; (*b*) and (*c*) coordination geometries around U2 and U1, respectively. Symmetry codes are defined in Table 2.

Table 3
Hydrogen bond geometry (Å, °) for (I).

D	H···*A*	*D* H	H···*A*	*D*···*A*	*D* H···*A*
N1	H1*Z*···$F1^{v}$	0.95 (1)	1.81 (3)	2.705 (5)	157 (5)
O3	H3*Z*···O6*W*	0.96 (1)	2.19 (2)	3.139 (13)	175 (6)
O3	H3*Z*···O7*W*	0.96 (1)	1.70 (2)	2.643 (13)	171 (5)
O8	H8*Y*···O4*W*	0.95 (1)	1.88 (4)	2.802 (10)	163 (13)
O8	H8*Y*···O5*W*	0.95 (1)	1.62 (3)	2.560 (13)	171 (14)
O8	H8*X*···O8*W*	0.95 (1)	1.90 (2)	2.850 (11)	176 (13)
O8	H8*X*···O9*W*	0.95 (1)	2.48 (3)	3.415 (17)	170 (12)

Symmetry code: (v) $x+\frac{1}{2}, y+\frac{1}{2}$, $z+\frac{1}{2}$.

Table 4
Selected bond lengths and angles (Å, °) for the U^{6+} coordination environments in (II).

U1	O4	1.781 (3)	U1	O1	2.278 (3)
U1	$O3^{ii}$	2.269 (4)			
O4	U1 $O4^{i}$	180	$O3^{ii}$	U1 O1	88.95 (14)
O4	U1 $O3^{ii}$	90.25 (15)	$O3^{iii}$	U1 O1	91.05 (14)
O4	U1 $O3^{ii}$	89.75 (15)	O4	U1 $O1^{i}$	90.07 (15)
$O3^{ii}$	U1 $O3^{iii}$	180	O1	U1 $O1^{i}$	180
O4	U1 O1	89.93 (15)			

Symmetry codes: (i) $x+1$, y, $z+2$; (ii) x, $y+\frac{1}{2}, z+\frac{1}{2}$; (iii) $x+1, y$ $\frac{1}{2}$, $z+\frac{3}{2}$.

hedron around U1 are occupied by a coordinated water molecule and four O atoms from the organic ligands. The bond lengths are 1.764 (4) and 1.769 (4) Å for U1 = O, 2.510 (4) Å for U1 O_{water} and in the range 2.323 (4) 2.368 (4) Å for U1 $O_{phosphonate}$. The mean plane formed by the equatorial atoms and the metal centre [largest deviation of 0.245 (4) Å for O4] subtends angles with the axial U═O bonds of 88.45 (16) and 89.26 (16)°. The equatorial *cis* O U1 O angles range from 65.24 (13) to 78.94 (13) ° (Fig. 1*c*). The coordination environment around U2 resembles a centrosymmetric bimetallic cluster bridged by two crystallographically equivalent fluoride anions. The remaining three equatorial positions are occupied by O atoms belonging to the organic ligands. The bonding distances are 1.767 (4) and 1.770 (4) Å for U2═O, between 2.307 (3) and 2.355 (3) Å for U2 $O_{phosphonate}$, and 2.336 (3) and 2.351 (3) Å for U2 F. The U···U distance in the dimer is 3.9829 (3) Å. The mean plane formed by the equatorial atoms and the metal centre [largest deviation of 0.037 (3) Å for F1] subtends angles with the axial U═O bonds of 88.48 (15) and 89.44 (15)°. The equatorial *cis* O U1 O angles range from 63.63 (11) to 79.44 (12)° (Fig. 1*b*). The organic residue H_3nmp^{3-} is coordinated to six metal centres, with one of the phosphonate groups coordinated to the metal as a μ_3-O,O′,O″-ligand, and the two PO_3H groups as μ_2-O,O′-ligands. The remaining charge-balancing proton is bonded to the central N1 atom.

As the structure does not show any noticeable void volume, we conclude that all of the water molecule sites in the crystal structure have been found. These molecules are, however, included with fractional site occupancies, and their H atoms could not be located from difference Fourier maps. This means that the water molecules are loosely located and suffer from

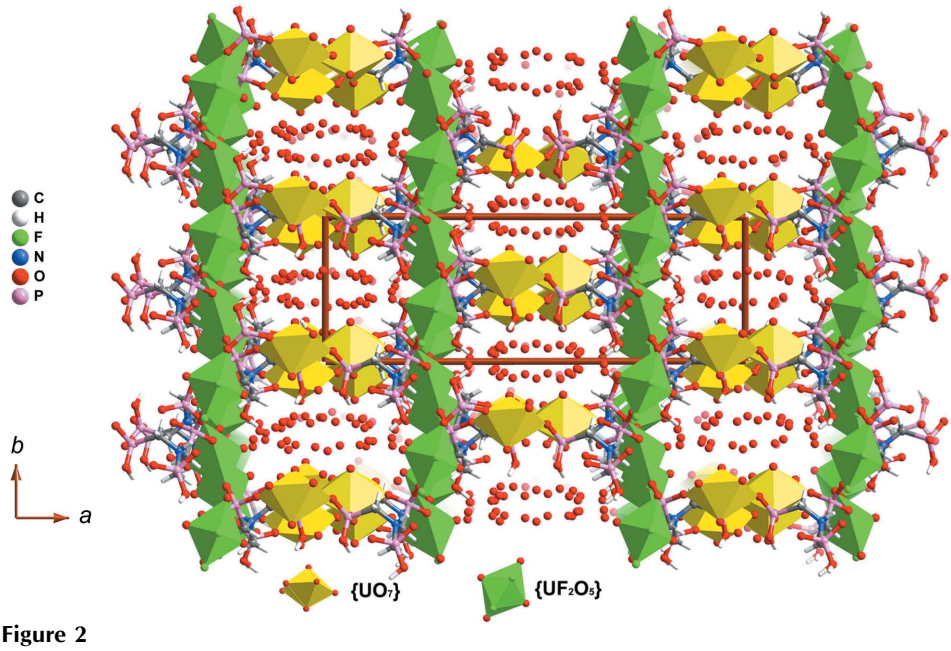

Figure 2
Crystal packing of (I) viewed along the [001] direction. The metal centres are represented as green or yellow polyhedra, depending on whether their coordination environment contains F atoms. H atoms of the water molecules were not located and, for this reason, the water molecules appear as isolated O atoms.

spatial and conformational disorder, and for this reason the hydrogen-bond network cannot be described completely. The interaction N1 H1*Z*···F1 is the only hydrogen bond with an unequivocal connection between a donor and an acceptor.

While the O3 atom donates its H atom to a pair of close, and fractionally occupied, water molecules, atom O8 appears to be connected to two half-occupied H atoms, with these being donated to two pairs of close and fractionally occupied water molecules (see Table 3 and Fig. 1 for details). The water molecules occupy a continuous column parallel to the *c* direction of the unit cell (Fig. 2). This column has a cross section of *ca* 10 × 5 Å^2, accounting for *ca* 23.6% of the total volume of the unit cell (*ca* 932 Å^3).

3.2. Crystal structure of [(UO$_2$)(H$_2$pmd)] (II)

Compound (II) crystallizes in space group $P2_1/c$, with the asymmetric unit being composed of half a 1,4-phenylenebis(methylene)diphosphonic acid ligand (H_2pmd^{2-}), a U^{6+} metal centre occupying an inversion centre, and one oxo ligand (Fig. 3*a*). The coordination geometry around the centrosymmetric metal centre resembles an octahedron squeezed along the axis defined by the crystallographically equivalent oxo ligands (Fig. 3*b*). The remaining positions of the coordination environment are occupied by four O atoms from the organic ligands. The bond lengths are 1.781 (3) Å for U1═O, and 2.269 (4) and 2.278 (3) Å for U1 $O_{phosphonate}$. While the equatorial *cis* octahedral O U1 O angles range from 88.95 (14) to

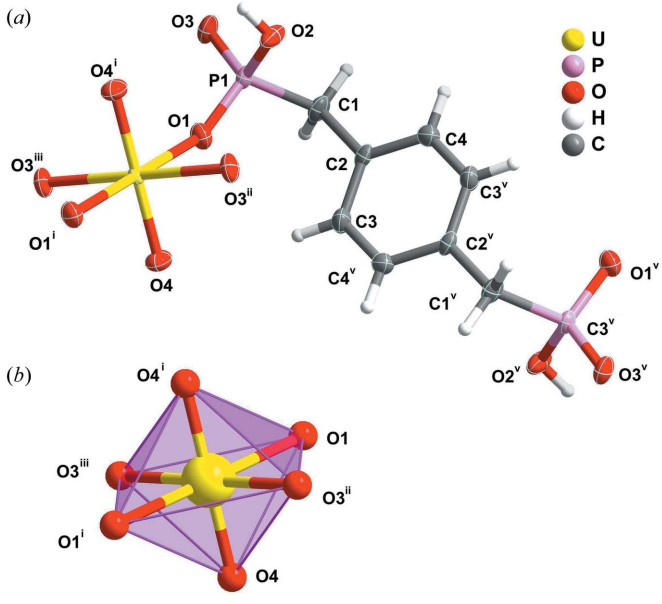

Figure 3
(*a*) Molecular units in (II). Non H atoms are represented as displacement ellipsoids at 50% probability, while H atoms are represented as small spheres with arbitrary radii; (*b*) coordination geometry around the metal centre. Symmetry codes are defined in Table 4, and: (v) $x+2$, y, $z+2$.

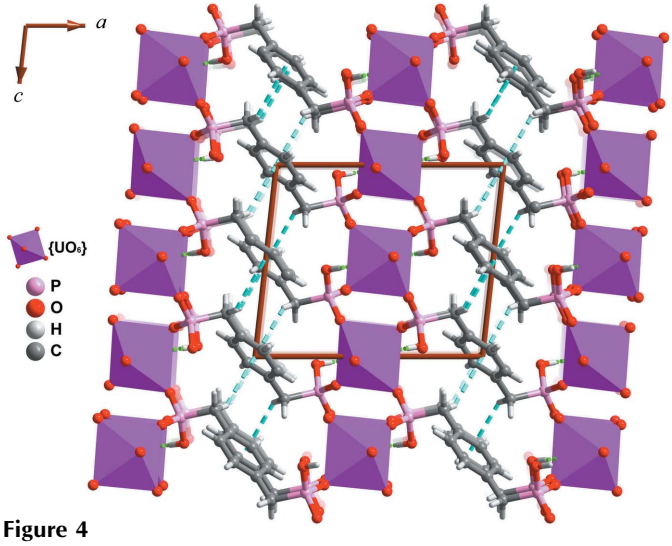

Figure 4
Crystal packing of (II) viewed along the [010] direction. Metal centres are represented as rose coloured squeezed octahedra. O H O and C H π interactions are depicted as green and blue dashed lines, respectively.

Table 5
Hydrogen bond geometry (Å, °) for (II).

D H···*A*	*D* H	H···*A*	*D*···*A*	*D* H···*A*
O2 H2*Z*···O4^{iv}	0.83 (1)	1.88 (2)	2.703 (5)	168 (5)
C1 H1*B*···*Cg*	0.97	2.86	3.588 (5)	133

Cg is the centroid of the ring composed by the atoms C2^{vi}, C3^{vi}, C4^{vi}, C2^{vii}, C3^{vii} and C4^{vii}. Symmetry codes: (iv) $x, y+1, z$; (vi) $x, \quad y+\frac{1}{2}, z \quad \frac{1}{2}$; (vii) $x+2, y+\frac{1}{2}, \quad z+\frac{3}{2}$.

Table 6
Selected bond lengths and angles (Å, °) for the U^{6+} coordination environments in (III).

U1	O10	1.774 (3)	U2	O8^{ii}	2.316 (3)
U1	O1	2.294 (3)	U2	O4^{iii}	2.324 (3)
U1	O5^{i}	2.307 (3)	U2	O9^{iv}	2.326 (3)
U2	O12	1.765 (3)	U2	O2	2.392 (3)
U2	O11	1.769 (3)	U2	O1*W*	2.472 (3)
O10	U1 O10^{v}	180	O11	U2 O9^{iv}	93.96 (12)
O10	U1 O1	91.00 (12)	O8^{ii}	U2 O9^{iv}	76.92 (10)
O10	U1 O1^{v}	89.00 (12)	O4^{iii}	U2 O9^{iv}	77.17 (10)
O1	U1 O1^{v}	180	O12	U2 O2	91.82 (12)
O10	U1 O5^{i}	89.89 (12)	O11	U2 O2	87.43 (12)
O1	U1 O5^{i}	88.08 (11)	O8^{ii}	U2 O2	132.79 (10)
O10	U1 O5^{iii}	90.11 (12)	O4^{iii}	U2 O2	73.10 (10)
O1	U1 O5^{iii}	91.92 (11)	O9^{iv}	U2 O2	150.20 (10)
O5^{i}	U1 O5^{iii}	180	O12	U2 O1*W*	85.23 (13)
O12	U2 O11	179.23 (14)	O11	U2 O1*W*	94.61 (13)
O11	U2 O8^{ii}	85.65 (13)	O8^{ii}	U2 O1*W*	68.03 (10)
O12	U2 O4^{iii}	90.71 (13)	O4^{iii}	U2 O1*W*	138.80 (11)
O11	U2 O4^{iii}	88.91 (13)	O9^{iv}	U2 O1*W*	143.08 (11)
O8^{ii}	U2 O4^{iii}	153.07 (10)	O2	U2 O1*W*	66.10 (10)
O12	U2 O9^{iv}	86.61 (12)			

Symmetry codes: (i) $x+1, y, z$; (ii) $x, \quad y, \quad z+1$; (iii) $x, \quad y+1, \quad z+1$; (iv) $x, y, z \quad 1$; (v) $x+1, \quad y+1, \quad z+1$.

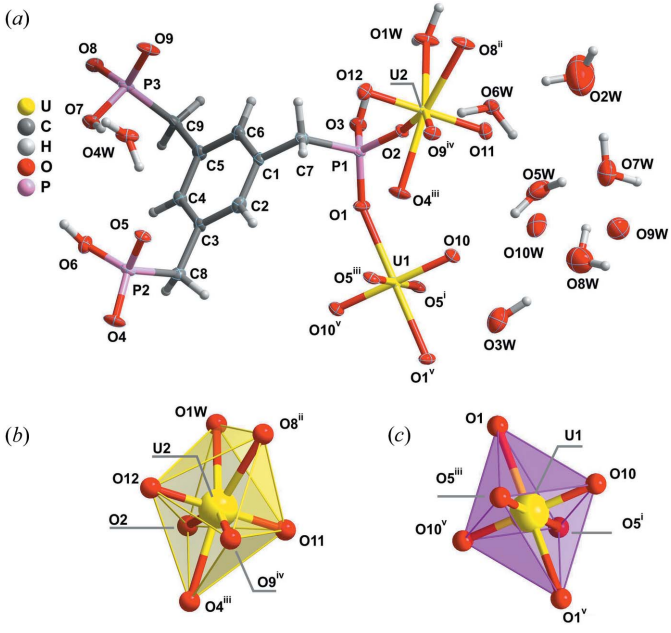

Figure 5
(*a*) Molecular units in (III). Non H atoms are represented as displace ment ellipsoids at 50% probability, while H atoms are represented as small spheres with arbitrary radii; (*b*) and (*c*) coordination geometries around U2 and U1, respectively. Symmetry codes as in Table 6.

Table 7
Hydrogen bond geometry (Å, °) for (III).

D H···*A*	*D* H	H···*A*	*D*···*A*	*D* H···*A*
O3 H3*Z*···O6*W*^{vi}	0.94 (1)	1.69 (1)	2.625 (4)	168 (4)
O6 H6*Z*···O3*W*^{iii}	0.94 (1)	1.68 (1)	2.609 (5)	168 (4)
O7 H7*Z*···O4*W*	0.94 (1)	1.76 (1)	2.696 (4)	171 (5)
O1*W* H1*X*···O6*W*^{vi}	0.95 (1)	1.80 (1)	2.747 (4)	173 (4)
O1*W* H1*Y*···O4*W*^{ii}	0.95 (1)	1.86 (2)	2.752 (5)	156 (5)
O2*W* H2*X*···O7*W*^{vii}	0.95 (1)	2.18 (6)	3.002 (9)	144 (8)
O2*W* H2*Y*···O11	0.95 (1)	2.15 (5)	3.010 (8)	150 (9)
O3*W* H3*X*···O8*W*	0.95 (1)	1.85 (1)	2.799 (7)	175 (4)
O3*W* H3*Y*···O10	0.95 (1)	2.67 (4)	3.336 (5)	128 (4)
O3*W* H3*Y*···O1^{v}	0.95 (1)	2.59 (3)	3.333 (5)	136 (3)
O4*W* H4*X*···O3^{viii}	0.95 (1)	1.95 (2)	2.841 (5)	156 (4)
O4*W* H4*Y*···O5	0.95 (1)	2.12 (2)	3.031 (4)	161 (4)
O5*W* H5*X*···O10	0.95 (1)	2.07 (2)	2.989 (5)	163 (4)
O5*W* H5*Y*···O7*W*	0.95 (1)	1.87 (1)	2.823 (7)	174 (3)
O6*W* H6*X*···O5*W*	0.94 (1)	1.73 (2)	2.645 (5)	164 (3)
O6*W* H6*Y*···O2	0.95 (1)	1.93 (1)	2.875 (4)	175 (4)
O7*W* H7*X*···O2*W*	0.95 (1)	1.81 (2)	2.741 (10)	163 (6)
O7*W* H7*Y*···O9^{ix}	0.95 (1)	2.04 (2)	2.972 (6)	166 (6)
O8*W* H8*X*···O7*W*	0.95 (1)	1.99 (3)	2.927 (8)	167 (9)
O8*W* H8*Y*···O3*W*^{x}	0.96 (1)	2.07 (5)	2.901 (8)	145 (7)

Symmetry codes: (ii) $x, \quad y, \quad z+1$; (iii) $x, \quad y+1, \quad z+1$; (v) $x+1, \quad y+1, \quad z+1$; (vi) $x+1, \quad y, \quad z+1$; (vii) $x+1, \quad y, \quad z$; (viii) $x \quad 1, y, z$; (ix) $x+1, y, z \quad 1$; (x) $x+1, \quad y+1, \quad z$.

91.05 (14)°, the *trans* octahedral angles are exactly 180° due to the location of the metal centre at the inversion centre (see Table 4 for details). The centrosymmetric organic residue H_2pmd^{2-} is coordinated to four metal centres with each PO_3H group acting as a μ_2-O,O′ ligand between two such centres. Compound (II) does not show any porosity, and its supramolecular interactions are limited to the O2 H2*Z*···O4 hydrogen bond and to C H···π interactions (see Table 5 and Fig. 4 for details).

3.3. Crystal structure of $[(UO_2)_3(H_3bmt)_2(H_2O)_2]\cdot 14H_2O$ (III)

Compound (III) crystallizes in space group $P\bar{1}$, with the asymmetric unit being composed of a whole residue of (benzene-1,3,5-triyltris(methylene))triphosphonic acid (H_3bmt^{3-}), one and a half crystallographically independent uranyl centres, a coordinated water molecule, and seven water molecules distributed over nine distinct crystallographic sites (Fig. 5*a*). Notably, even though the crystallization of (III) could only be achieved with the addition of HF to the reaction mixture [as for compound (I), see §2], fluoride anions do not seem to be included in the crystal structure. Elemental analysis on representative amounts of the isolated compound strongly point to the absence of fluoride anions (see §2). In addition, no crystallographic evidence was found for the presence of fluoride anions.

The coordination environments around the two metal centres are different: while that of U1 resembles a squeezed centrosymmetric octahedron similar to that in compound (II) (Fig. 5*b*), the coordination environment of U2 bears strong similarities to the pentagonal bipyramid around U1 in compound (I) (Fig. 5*c*). The bond lengths around U2 are 1.765 (3) and 1.769 (3) Å for U2═O, 2.472 (3) Å for

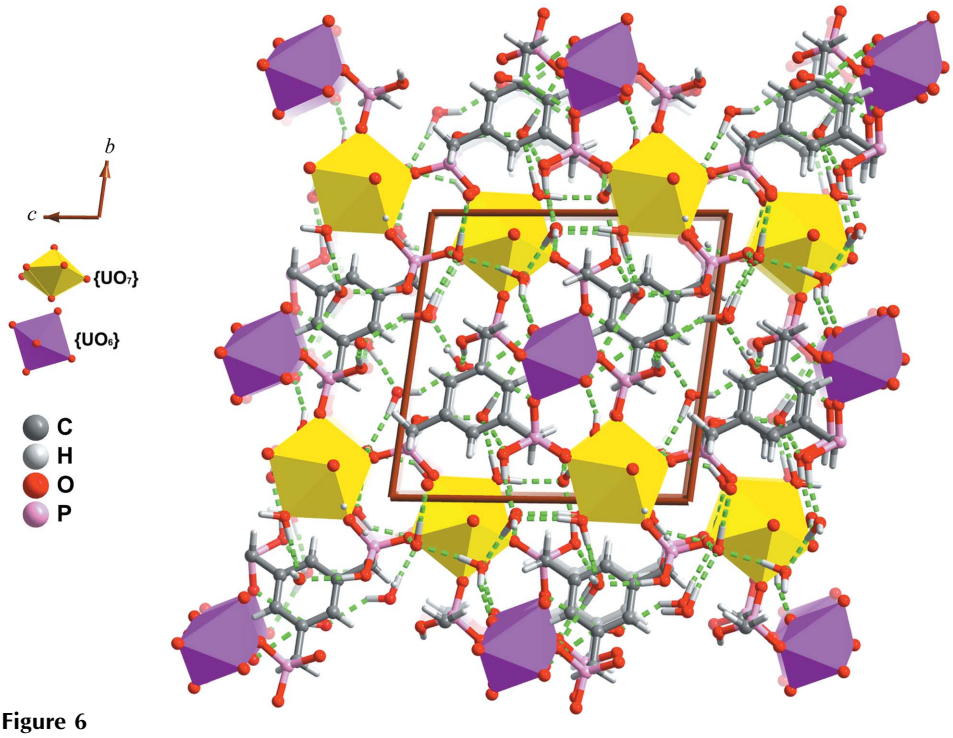

Figure 6
Crystal packing of (III) viewed along the [100] direction. Metal centres are represented as rose or yellow polyhedra, for octahedral or pentagonal bipyramidal geometries, respectively. O H O interactions are depicted as dashed green lines. Crystallization water molecules with low site occupancy (O9*W* and O10*W*) have been omitted for clarity.

U2 O_{water} and in the range 2.316 (3) 2.392 (3) Å for U2 $O_{phosphonate}$. The mean plane formed by the equatorial atoms and the metal centre [largest deviation 0.205 (4) Å for O8] subtends angles with the axial U═O bonds of 89.37 (15) and 89.80 (15)°. The equatorial *cis* O U2 O angles range from 66.10 (10) to 77.17 (10)°. For the U1 environment, the bond lengths are 1.774 (3) for U1═O, and 2.294 (4) and 2.307 (3) Å for U1 $O_{phosphonate}$. The equatorial *cis* octahedral O U1 O angles range from 88.08 (11) to 91.92 (11)° (see Table 6 for details). The organic residue H_3bmt^{3-} is coordinated to six metal centres, with all of the PO_3H groups coordinating to the metal as μ_2-O,O′-ligands.

The water molecules occupy a continuous zigzag layer parallel to the (100) planes of the unit cell, occupying *ca* 26.9% of the total cell volume (*ca* 335 Å). The considerable number of donor and acceptor atoms contributes to the existence of a complex network of hydrogen bonds, showing rings with graph-set motifs $R_4^4(8)$ (two), $R_4^4(8)$, $R_5^3(10)$, $R_8^6(16)$, $R_8^7(17)$ and $R_{12}^8(23)$ (Grell *et al.*, 1999; see Table 7 and Fig. 6 for additional details).

3.4. FT-IR spectroscopy

FT-IR spectroscopy on representative amounts of (I) (III) show the most important diagnostic bands attributed to the functional groups composing the organic ligands (Fig. 7). Due to the low wavenumbers in which the U F vibrational modes appear (typically below 300 cm^{-1}) these bands could not be used to establish unequivocally the absence of fluoride anions in the structure of compound (III).

The FT-IR spectra of (I) and (III) show very broad bands in the range 3600 3200 cm^{-1} attributed to the ν(O H) stretching modes of the coordinated water molecules. The in-plane deformation $\delta(H_2O)$ bands of the water molecules are also clearly visible in the range *ca* 1650 1600 cm^{-1}. All of these bands are, as expected, absent from the spectrum of (II). The bands found between *ca* 3200 2800 cm^{-1} are attributed to the typical symmetric and asymmetric ν(C H) stretching vibrational modes, being much more visible for (II) due to the absence of the aforementioned broad band from the water molecules. The absence of water in (II) also permits observation in much more detail of the typical ν(PO H) stretching vibrational mode at *ca* 3160 cm^{-1} (Fig. 7).

As we have reported previously for lanthanide-containing MOF structures with H_4pmd ligands (Vilela *et al.*, 2014), the combination of $\delta(CH_2)$ and ν(Ph) vibrational modes in the *ca* 1520 1400 cm^{-1} spectral region is markedly visible in the spectrum of (II) due to the appearance of sharp strong bands which are typically absent from the remaining materials, particularly compound (I). The presence of this organic ligand is also notable as a strong broad band peaking at *ca* 870 cm^{-1}, attributed to a combination of the $\rho(CH_2)$ and γ(CH) modes (Vilela *et al.*, 2014). Below *ca* 1100 cm^{-1}, all spectra are strongly dominated by a multitude of bands arising from the phosphonate groups which overlap with the typical ν_3 asymmetric stretching vibrational mode of the uranyl, UO_2^{2+}, group.

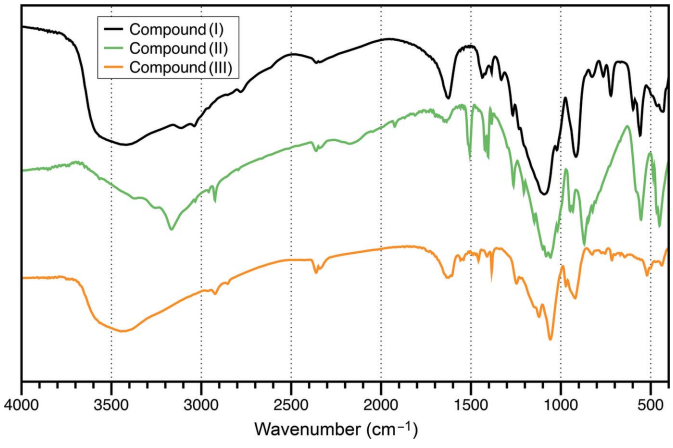

Figure 7
FT IR spectra of (I) (III) collected in the 400 4000 cm ^{1} range.

Particularly, between 1100 and 900 cm^{-1}, various bands are attributed to the $\nu(PO_3)$ modes of these groups, and at *ca* 580 and 554 cm^{-1}, two markedly visible bands in the spectrum of (II) arise from the combination of the $\delta(PO_3)$ and γ(Ph) modes.

4. Topological studies

The frameworks (I) (III) can be conveniently described by employing a topological approach (Baburin *et al.*, 2005; Blatov *et al.*, 2004). This simplification approach, purely based on mathematical concepts, consists of reducing each network into objects that structurally could be envisaged as central nodes and connecting bridges (between two or more individual nodes). All topological studies have been performed using the software package *TOPOS* (Blatov, 2012). From the structures of (I) (III) a number of common structural features can be discerned among the frameworks: (i) they are assembled from one or two crystallographically independent uranyl-based metal centres; (ii) they contain a single organic residue [or a fragment in the case of (II)] in their asymmetric units; (iii) the organic ligands make physical connections between the uranyl-based metal centres.

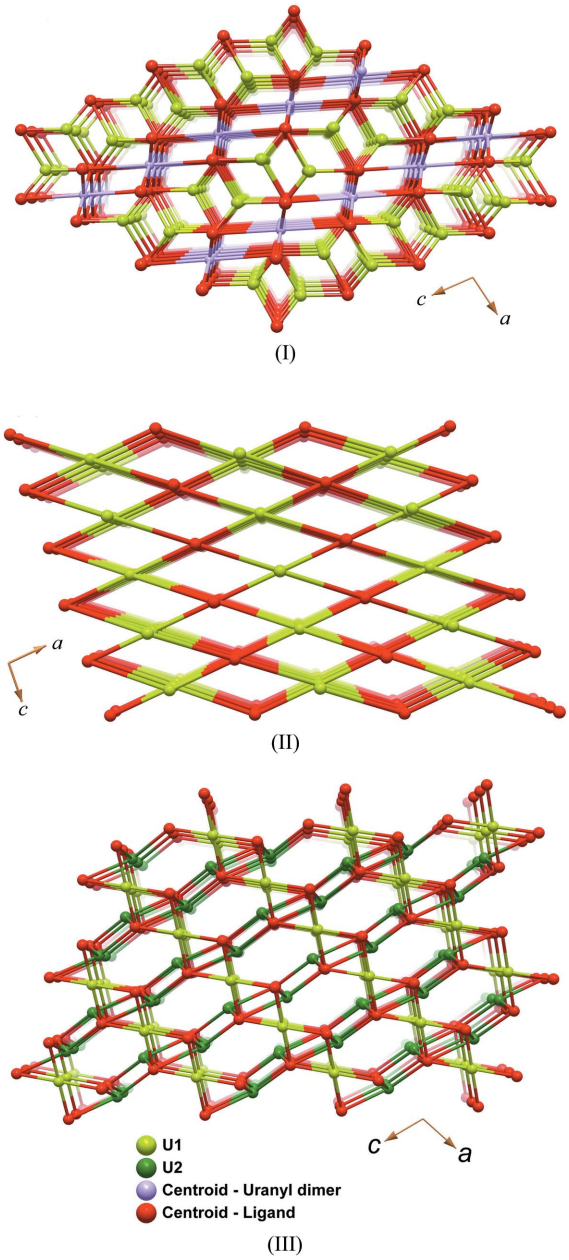

Figure 8
Topological representations of (I) (III).

Alexandrov *et al.* (2011) have considered that an organic ligand is of crucial structural importance in a framework when it establishes links between two or more metal centres (μ_n). This idea could be extended to other structurally important aggregates of atoms, such as the $\{(UO_2)O_3(\mu\text{-F})\}_2$ dimer present in (II) and formed by the crystallographically independent U2 centres (see detailed structure description above). Therefore, for the performed topological studies, the centroids of each organic ligand and of the $\{(UO_2)O_3(\mu\text{-F})\}_2$ dimer were taken as network nodes, along with the remaining uranyl metal centres. Two of the compounds are, in this way, trinodal: (I) is a 3,6,6-connected network with overall point symbol $\{4^3\}_2\{4^7\cdot6^7\cdot8\}_2\{4^8\cdot6^6\cdot8\}$, of which the $\{(UO_2)O_3(\mu\text{-F})\}_2$ dimer and the organic ligands are both six-connected nodes (Fig. 8*a*); (III) is instead a 4,4,6-connected network (point symbol: $\{4^2\cdot8^4\}\{4^4\cdot6^2\}_2\{4^9\cdot6^6\}_2$) having only the organic ligand as a six-connected node (Fig. 8*c*). While (III) has a known topology deposited within the *TOPOS* database (4,4,6T19), (I) corresponds to a new topological type. Searches in the Reticular Chemistry Structure Resource (RCSR; O'Keeffe *et al.*, 2008) and in *EPINET* (Hyde *et al.*, 2006) reveal that the nodal connectivity of compound (I) is, to the best of our knowledge, unprecedented among MOF structures.

Compound (II) is a much simpler network having only two nodes which are topologically identical: both the organic ligand and the uranyl group are 4-connected nodes with exactly identical coordination shells up to N_{10} (= 1489) (Fig. 8*b*). In this way, this network is 4-connected uninodal with point symbol $\{4^5\cdot8\}$ and topology identical to that of the $CdSO_4$ compound (type **cds**).

5. Conclusions

Three new MOF compounds based on uranyl groups coordinated to polyphosphonate-bearing ligands were isolated from hydrothermal synthesis and structurally characterized in the solid state. Compound (I) shows two different uranyl environments with pentagonal bipyramidal geometries, from which one comprises a centrosymmetric bimetallic cluster formed by two F^- bridges. In contrast to the previously prepared materials with lanthanides and the ligand H_6nmp, which comprised two-dimensional coordination polymers (Silva *et al.*, 2011; Cunha-Silva *et al.*, 2007), compound (I) comprises a highly porous three-dimensional network.

The coordination geometry around the uranyl group in (II) resembles a squeezed octahedron. The structure comprises layers of inorganic uranyl phosphonates alternating with organic layers composed by the hydrocarbon part of the

ligand. This resembles the packing observed in the previously prepared lanthanide materials with the same ligand (Vilela, Mendes *et al.*, 2013; Shi *et al.*, 2008). In contrast to these compounds (II) is fully dehydrated.

Compound (III) is based on two uranyl environments with different coordination geometries, one being a pentagonal bipyramid and the other a squeezed octahedron. In relation to the previously prepared compounds with H_6bmt and lanthanides (Vilela, Firmino *et al.*, 2013; Vilela *et al.*, 2012), compound (III) exhibits a considerably larger cavity occupied by a larger number of water molecules. While compounds (II) and (III) have known topological types, compound (I) corresponds to an unprecedented topological type among MOF structures.

We thank *Fundação para a Ciência e a Tecnologia* (FCT, Portugal), the European Union, QREN, FEDER, COMPETE and *Laboratório Associado Centro de Investigação em Materiais Cerâmicos e Compósitos*, CICECO (Pest C-CTM/LA0011/2013), the research unit QOPNA (PEst-C/QUI/UI0062/2013) for their general funding scheme. We further thank FCT for the R&D project PTDC/QUI-QUI/098098/2008 (FCOMP-01-0124-FEDER-010785), and for specific funding towards the purchase of a single-crystal diffractometer. We are also grateful to FCT for the PhD grant No. SFRH/BD/66371/2009 (to SMFV) and the post-doctoral grants SFRH/BPD/47087/2008 (to BM) and SFRH/BPD/63736/2009 (to JAF).

References

Adelani, P. O., Oliver, A. G. & Albrecht Schmitt, T. E. (2011). *Cryst. Growth Des.* **11**, 3072 3080.
Alexandrov, E. V., Blatov, V. A., Kochetkov, A. V. & Proserpio, D. M. (2011). *CrystEngComm*, **13**, 3947 3958.
Almeida Paz, F. A., Shi, F. N., Klinowski, J., Rocha, J. & Trindade, T. (2004). *Eur. J. Inorg. Chem.* pp. 2759 2768.
Almeida Paz, F. A., Rocha, J., Klinowski, J., Trindade, T., Shi, F. N. & Mafra, L. (2005). *Prog. Solid State Chem.* **33**, 113 125.
Alsobrook, A. N., Alekseev, E. V., Depmeier, W. & Albrecht Schmitt, T. E. (2011). *Cryst. Growth Des.* **11**, 2358 2367.
Andrews, M. B. & Cahill, C. L. (2013). *Chem. Rev.* **113**, 1121 1136.
Baburin, I. A., Blatov, V. A., Carlucci, L., Ciani, G. & Proserpio, D. M. (2005). *J. Solid State Chem.* **178**, 2452 2474.
Blatov, V. A. (2012). *Struct. Chem.* **23**, 955 963.
Blatov, V. A., Carlucci, L., Ciani, G. & Proserpio, D. M. (2004). *CrystEngComm*, **6**, 377 395.
Brandenburg, K. (2009). *DIAMOND*. Crystal Impact GbR, Bonn, Germany.
Bruker (2008). *APEX2, SADABS, SAINT Plus* and *SHELXTL*. Bruker AXS, Madison, Wisconsin, USA.
Cunha Silva, L., Ananias, D., Carlos, L. D., Almeida Paz, F. A. & Rocha, J. (2009). *Z. Kristallogr.* **224**, 261 272.
Cunha Silva, L., Lima, S., Ananias, D., Silva, P., Mafra, L., Carlos, L. D., Pillinger, M., Valente, A. A., Paz, F. A. A. & Rocha, J. (2009). *J. Mater. Chem.* **19**, 2618 2632.
Cunha Silva, L., Mafra, L., Ananias, D., Carlos, L. D., Rocha, J. & Almeida Paz, F. A. (2007). *Chem. Mater.* **19**, 3527 3538.
Grell, J., Bernstein, J. & Tinhofer, G. (1999). *Acta Cryst.* B**55**, 1030 1043.
Hyde, S. T., Delgado Friedrichs, O., Ramsden, S. J. & Robins, V. (2006). *Solid State Sci.* **8**, 740 752.
Kottke, T. & Stalke, D. (1993). *J. Appl. Cryst.* **26**, 615 619.
O'Keeffe, M., Peskov, M. A., Ramsden, S. J. & Yaghi, O. M. (2008). *Acc. Chem. Res.* **41**, 1782 1789.
Oxford Cryosystems (2006). *Cryopad*. Oxford Cryosystems Ltd, Oxford, England.
Rocha, J., Paz, F. A. A., Shi, F. N., Ferreira, R. A. S., Trindade, T. & Carlos, L. D. (2009). *Eur. J. Inorg. Chem.* pp. 4931 4945.
Sheldrick, G. M. (2008). *Acta Cryst.* A**64**, 112 122.
Shi, F. N., Paz, F. A. A., Girginova, P. I., Amaral, V. S., Rocha, J., Klinowski, J. & Trindade, T. (2006). *Inorg. Chim. Acta*, **359**, 1147 1158.
Shi, F. N., Paz, F. A. A., Girginova, P. I., Rocha, J., Amaral, V. S., Klinowski, J. & Trindade, T. (2006). *J. Mol. Struct.* **789**, 200 208.
Shi, F. N., Trindade, T., Rocha, J. & Paz, F. A. A. (2008). *Cryst. Growth Des.* **8**, 3917 3920.
Silva, P., Fernandes, J. A. & Almeida Paz, F. A. (2012). *Acta Cryst.* E**68**, m294 m295.
Silva, P., Vieira, F., Gomes, A. C., Ananias, D., Fernandes, J. A., Bruno, S. M., Soares, R., Valente, A. A., Rocha, J. & Paz, F. A. (2011). *J. Am. Chem. Soc.* **133**, 15120 15138.
Soares Santos, P. C., Cunha Silva, L., Paz, F. A., Ferreira, R. A., Rocha, J., Carlos, L. D. & Nogueira, H. I. (2010). *Inorg. Chem.* **49**, 3428 3440.
Thuéry, P. (2013). *Cryst. Growth Des.* **52**, 435 447.
Thuéry, P., Masci, B. & Harrowfield, J. (2013). *Cryst. Growth Des.* **13**, 3216 3224.
Vilela, S. M. F., Ananias, D., Fernandes, J. A., Silva, P., Gomes, A. C., Silva, N. J. O., Rodrigues, M. O., Tomé, J. P. C., Valente, A. A., Ribeiro Claro, P., Carlos, L. D., Rocha, J. & Almeida Paz, F. A. (2014). *J. Mater. Chem. C*, doi: 10.1039/c3tc32114*b*.
Vilela, S. M. F., Ananias, D., Gomes, A. C., Valente, A. A., Carlos, L. D., Cavaleiro, J. A. S., Rocha, J., Tomé, J. P. C. & Almeida Paz, F. A. (2012). *J. Mater. Chem.* **22**, 18354 18371.
Vilela, S. M. F., Firmino, A. D. G., Mendes, R. F., Fernandes, J. A., Ananias, D., Valente, A. A., Ott, H., Carlos, L. D., Rocha, J., Tomé, J. P. C. & Almeida Paz, F. A. (2013). *Chem. Commun.* **49**, 6400 6402.
Vilela, S. M. F., Mendes, R. F., Silva, P., Fernandes, J. A., Tomé, J. P. C. & Paz, F. A. A. (2013). *Cryst. Growth Des.* **13**, 543 560.